



City Research Online

City, University of London Institutional Repository

Citation: Rajana, K., Alonso-Rodríguez, A. & Tsavdaridis, K. D. (2021). A wavelet-based approach for describing the mechanical behaviour of cellular beams. *Steel Construction*, 14(1), pp. 47-54. doi: 10.1002/stco.202000043

This is the accepted version of the paper.

This version of the publication may differ from the final published version.

Permanent repository link: <https://openaccess.city.ac.uk/id/eprint/27677/>

Link to published version: <https://doi.org/10.1002/stco.202000043>

Copyright: City Research Online aims to make research outputs of City, University of London available to a wider audience. Copyright and Moral Rights remain with the author(s) and/or copyright holders. URLs from City Research Online may be freely distributed and linked to.

Reuse: Copies of full items can be used for personal research or study, educational, or not-for-profit purposes without prior permission or charge. Provided that the authors, title and full bibliographic details are credited, a hyperlink and/or URL is given for the original metadata page and the content is not changed in any way.

City Research Online:

<http://openaccess.city.ac.uk/>

publications@city.ac.uk

1 Komal Rajana, Andrés Alonso-Rodríguez, Konstantinos Daniel Tsavdaridis

A Wavelet-Based Approach for Describing the Mechanical Behaviour of Cellular Beams

Comments

This paper describes how a wavelet model comprised of a linear combination of sine terms is capable of representing the cross-section inertia variation along the length of cellular beams. This allows for the efficient computation of deflections of cellular beams while being deployed as part of steel-concrete composite flooring systems, without considering purely statistical approaches or piece-wise integration of moment-curvature relationships that lead to cumbersome matrix approaches that complicate the assessment of deflections. Despite its simplicity, the proposed approach is found to be reliable as it successfully predicts displacements obtained through finite element model representations of more than 260 cases with errors smaller than $\pm 5\%$. Furthermore, the proposed analytical description of cross-section inertia along the beam length is defined by only three parameters that can be inferred through linear expressions considering the geometrical characteristics of a perforated beam - namely the ratio of flange and web thicknesses, the second moment of inertia of the steel beam, and the ratio between beam length and its depth, making it easy for widespread application by practitioners.

Keywords: Cellular beams; Perforated beams; Variable Inertia; Wavelets; Structural Steel Design

Ein Wavelet-basierter Ansatz zur Beschreibung des mechanischen Verhaltens von Kassettenbalken:
In diesem Artikel wird beschrieben, wie ein Wavelet-Modell, das aus einer linearen Kombination von Sinus-Termen besteht, die Trägheitsvariation des Querschnitts entlang der Länge der Zellstrahlen darstellen kann. Dies ermöglicht die effiziente Berechnung von Durchbiegungen von Zellenträgern, während sie als Teil von Stahl-Beton-Verbundbodensystemen eingesetzt werden, ohne rein statistische Ansätze oder die stückweise Integration von Moment-Krümmungs-Beziehungen zu berücksichtigen, die zu umständlichen Matrixansätzen führen, die die Bewertung von Durchbiegungen erschweren. Trotz seiner Einfachheit hat sich der vorgeschlagene Ansatz als zuverlässig erwiesen, da er Verschiebungen, die durch Finite-Elemente-Modelldarstellungen von mehr als 260 Fällen mit Fehlern von weniger als $\pm 5\%$ erhalten wurden, erfolgreich vorhersagt. Darüber hinaus wird

Comments

die vorgeschlagene analytische Beschreibung der Querschnittsträgheit entlang der Trägerlänge durch nur drei Parameter definiert, die durch lineare Ausdrücke unter Berücksichtigung der geometrischen Eigenschaften eines perforierten Trägers abgeleitet werden können - nämlich das Verhältnis von Flansch- und Stegdicken, das zweite Moment von der Trägheit des Stahlträgers und das Verhältnis zwischen Trägerlänge und -tiefe, und so die breite Anwendung durch Praktiker erleichtern.

Stichworte: Kassettenbalken; Perforiertebalken; Variable Trägheit; Wavelet; Stahlbau Bemessung

2 INTRODUCTION

Sustainable development is becoming a major concern worldwide, leading to a re-evaluation of current practices to ensure that current needs do not compromise the well-being of future generations [1]. Particularly, a new development approach, the Doughnut framework, is becoming mainstream [2]. It calls for implementing industrial processes that limit energy and resource consumption within a band that effectively satisfy basic needs for a comfortable life without depleting the capability of the environment to replenish, requiring a highly optimal use of basic goods [3].

Steel Construction has a high adverse environmental impact, as the production of new structural steel has been estimated to produce between 1.85 tonnes of equivalent CO₂ per tonne of structural steel, making the steel industry responsible for the 8% of total CO₂ emissions related to the use of fossil fuels worldwide, according to the World Steel Association [4]. Even if extensive recycling is implemented, the challenge ahead is daunting as a large investment in infrastructure, estimated between 7 to 9 USD Trillion, is required to be allocated by 2040 [5]. Consequently, current practices would lead to a disproportionate impact on the natural environment that would make the development of new infrastructure non-sustainable.

This calls for more efficient use of structural steel in the construction industry. One interesting approach is the use of perforated steel beams that use less material and minimize the self-weight of structures. Furthermore, openings in girders and beams facilitate other construction tasks, particularly the installation of ventilation, electricity, and data networks, leading to further resource and time savings. Also, it has been observed that the widespread use of perforated beams allows for larger free spans, leading to more ventilated, light-filled spaces that require installation of a lower number of structural columns, making their deployment even more sustainable and cost-rational.

Review

Comments

Comments

The design of perforated steel beams is more challenging than procedures for beams without openings as several intricate behavioural patterns are introduced by creating openings in the web region. The discontinuities in the beam web compromise the validity of Euler's plane theory [6], and lead to localised failure modes like flange buckling and torsion as well as large section warping [7a], preventing the stable achievement of substantial plastification of the cross-section, resulting in significant degradation of potential structural capacity. However, most of these issues have been addressed by research to some extent, leading to perforated beam designs that are cost-efficient and are capable of reaching a structural capacity comparable to their unperforated counterparts [8,9]. Several perforation shapes have been assessed among them circular [10]; hexagonal and octagonal [7a, 11]; elliptical [12], and topologically optimized [13]; even use perforated H beams has been explored [14], while Tsavdaridis and Galiatsatos addressed [15] the issue of the optimal placing of stiffeners. Most recently, research and development about cellular beams is trending towards the reduction of the overall thickness of floor systems leading to diverse solutions, among them: Ultra Shallow Floor Beams (USFB) [16] where at least the top flange is completely encased within the concrete slab; Composite Slim Floor Beams (CoSFB) that fit hollow core planks between flanges [17]; and, Delta Composite Beams that consider a perforated prismatic element with a trapezoidal cross-section. Its openings allow for continuity of reinforcement, if fully enclosed; or building services if only the top flange is embedded; making them convenient while achieving a notable fire-resistant behaviour [18]. Despite these research outcomes; current established design guidelines still underestimate the structural capacity of most widely used configurations of perforated beams by at least 15% and 40% at most [19], showcasing the need for developing tools that facilitate widespread adoption.

Also, web openings reduce the cross-section stiffness in a non-linear fashion along the beam length. Thus, it is expected that perforated beams experience larger deflections than beams without openings for the same loads [20]. This issue can become critical for the design, as it would compromise their function under serviceability conditions [21] due to fatigue and damage to non-structural elements, which have a deformation capacity within the elastic or nearly-elastic range less than a fifth to what is observed for structural components [22,23].

Therefore, reliable methods for assessing the deflections of perforated beams have been a pressing

need for engineering practice. Pioneering research on the topic was carried on in the 1970s [24]. The most common approach to address this issue is through direct integration of load-deflection relationships or using the virtual work method [25-29] considering discontinuous functions. This leads to formulation of matrices that must be solved for each particular case, leading to a proto-finite element model formulation that must be coupled with the general model of the whole structure for concise finite element model analyses. This level of complexity and lack of a way to establish general rules for quick design of floor systems, which is usually done separately from the assessment of the lateral load resisting frame, has limited widespread application by practitioners. Another approach to develop reliable methods for assessing deflections is to perform regression analyses on the results of finite element models [30], which could be easily applied to several cases. However, as relationships are statistical, the fundamental processes leading to them are obscured.

This paper aims to explore analytical expressions that are capable of describing the stiffness variation along length observed in composite-perforated beams. For that purpose, periodic expressions that are defined in non-dimensional scales are desired, being a prime candidate Wavelets [31]. Furthermore, they have been extensively used in signal analysis for filtering and signal compression [32], making engineers familiar with them. Therefore, this study modifies the Mavoreidis-Papageorgiou (MP) Wavelet [33] for representing the variation of flexural inertial along the length of a beam with circular, evenly-spaced openings, which are observed to have the best structural performance. This configuration leads to stable collapse mechanisms with a large deformation capacity that involves development of four plastic hinges around the openings [8,9]. The proposed function is a linear combination of sine functions that involves at most 4 parameters, which can be inferred directly from the geometry of the beam. Therefore, deflections along the beam can be found analytically through direct integration of moment-curvature relationships if the moment diagram is known. This approach has been benchmarked by finding the set of parameters that minimizes the squared difference between deflections predicted by the proposed stiffness variation and results of finite elements, focusing on locations centered along the mid-span and spreading two-thirds of the beam length from it in both directions. Results indicate that relative errors on deflection are less than 5% for more than 99% of all samples. As a consequence, the proposed stiffness variation is capable of providing insight into expected deflections of flooring systems, which are usually simply supported

on girders. Finally, reliable regression equations are provided, relating the beam geometry with parameters describing the stiffness variation of the beam, allowing for easy use by practitioners.

3 DEFLECTIONS OF SIMPLY SUPPORTED CELLULAR BEAMS WITH VARIABLE INERTIA

Euler's plane section hypothesis leads to a direct relationship between moment demands, flexural inertia, and deflection [34].

$$\frac{M(x)}{EI(x)} = \frac{d^2 u}{dx^2} \quad (1)$$

Where $M(x)$ is the moment demand along at ordinate x along the beam, E is the young's Modulus, and u is the deflection. For simply supported beams, $M(x)$ is given by:

$$M(x) = \frac{wL}{2}x - \frac{wx^2}{2} \quad (2)$$

Boundary conditions for a simply supported beam require that the deflection is zero at its extremes ($x = 0$ and $x = L$). After integrating Equation (1) twice and incorporating these conditions, the deflection is given by:

$$u(x) = \iint \frac{M(x)}{EI(x)} dx - \left(\int_0^L \frac{M(x)}{EI(x)} dx \right) x \quad (3)$$

The flexural inertia can be alternatively expressed as:

$$I(\xi) = EI_0 S(\xi) \quad (4)$$

After replacing Equation (2) into Equation (4) and introducing the accessory normalizing variable ξ , Equation (3) becomes:

$$u(\xi) = \frac{wL^4}{2EI_0} \left[\iint \frac{\xi - \xi^2}{S(\xi)} d\xi - \left(\int_0^1 \frac{\xi - \xi^2}{S(\xi)} d\xi \right) \xi \right] \quad (5)$$

ξ takes values between 0 and 1, $S(\xi)$ should have an oscillatory behaviour, capable of representing the effect of the changes of the inertia of the cross-section. Similarly, the proposed model should scale well with length, being versatile enough to accommodate a varying number of perforations. Wavelets are well suited for these purposes.

One of the most versatile wavelet models available is the MP acceleration pulse [33] Most recently, it was shown that it can be represented as the sum of three sine terms, making it differentiable and integrable to any order [35]. However, the function defining it cannot take negative values, compromising its suitability to represent $S(\xi)$ in its basic form. In this study, the MP pulse model has been tailored to fit the requirements of flexural stiffness variations in beams, leading to the following

expression

$$S(\xi, A_e, \kappa, \gamma) = A_e - \kappa \left\{ \left(\frac{\gamma+1}{2\gamma} \right) \sin[2\pi(\gamma+1)\xi - \pi\gamma] + \left(\frac{\gamma-1}{2\gamma} \right) \sin[2\pi(\gamma-1)\xi - \pi\gamma] - \sin(2\pi\gamma\xi - \pi\gamma) \right\}^2 ; 0 \leq \xi \leq 1 \quad (6)$$

A_e , κ and γ are parameters that have been observed in this study to depend on the geometry of the cellular beam, namely, its length, its flange and web widths, and the gross inertia of the cross-section EI_0 . Fig 1 shows plausible trends for $S(\xi, A_e, \kappa, \gamma)$ which have been observed for certain beam configurations considered in this study.

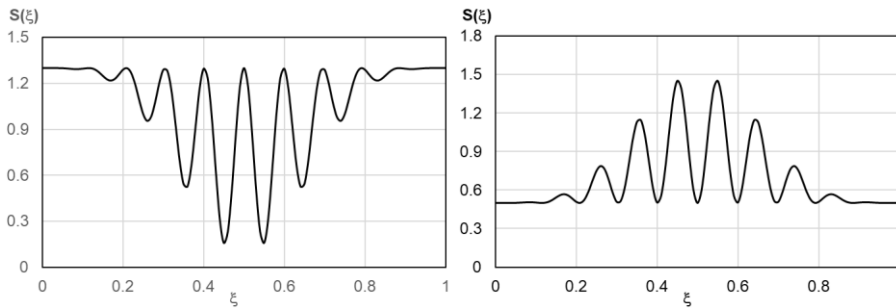


Fig 1. Examples of S . $A_e = 1.3$, $\kappa = 0.3$, $\gamma = 5$ on left; $A_e = 0.5$, $\kappa = 0.25$, $\gamma = 5$ on right.

Beispiele von S . $A_e = 1.3$, $\kappa = 0.3$, $\gamma = 5$ links; $A_e = 0.5$, $\kappa = 0.25$, $\gamma = 5$ rechts.

4 Methodology

Firstly, a set of benchmarking test cases were formulated, considering typical layouts for flooring systems expected in residential and light-retail properties. The base model consists of I beams 500mm deep and 200mm wide overlaid by a 100mm thick concrete slab. This arrangement is subjected to a load intensity of 50 kN/m. The layout of the benchmark cases follows the following limits on ratios between web height, opening diameter, and perforation center spacing, according to design guidelines [7]:

$$1.25 < \frac{H_w}{D_o} < 1.75 \quad (7)$$

$$1.08 < \frac{S_o}{D_o} < 1.5 \quad (8)$$

Thresholds defined in Equations (8,9) will prevent unexpected buckling and torsion of the web. Similarly, the first opening is made at a distance larger than one half of its diameter from each of its ends, to prevent crushing due to the reactions at its ends.

Review

Comments

Comments

Then the following variations were imposed on the base model; 1) beam lengths ranging between 2.2m and 6.8m; 2) Concrete slab widths equivalent to one fourth or the beam length, to account for composite action with the steel beam, following design recommendations [7]; 3) flange and web widths of 10, 15, and 20mm considering all their possible combinations; 4) hole spacing of 23, 27, 33, 116, and 200mm. The first three cases were grouped as closely-spaced perforations, while the last two were denominated average and widely-spaced perforations. A total of 267 test cases were defined, and they are summarized in the appendix (Table A.1), while a general layout of the geometrical characteristics of the specimens is presented in Fig 2.

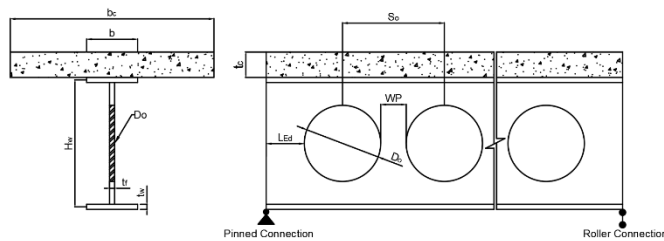
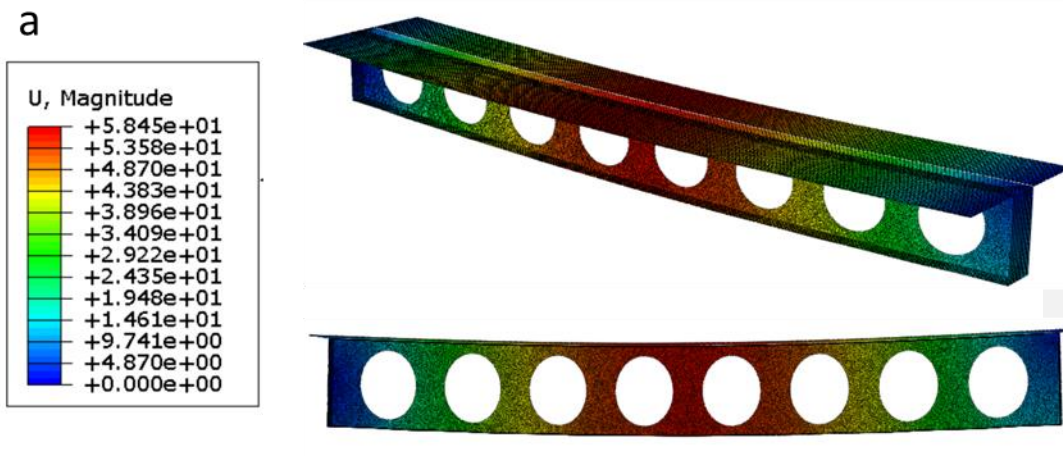


Fig. 2 Geometrical layout of test cases considered.

Geometrisches Anlage der berücksichtigten Testfälle.

Assessment of behavior of the test cases was done using the finite element method (FEM) implemented in Abaqus© [36] employing hexahedral, eight-node shell elements for both the concrete slab and the steel beam; having an aspect ratio less 2 and a largest dimension less than $h_w/20$ for elements placed between openings, following El -Sawhi et al. [37]. This arrangement has been observed to accurately describe observed behavior of composite beams during laboratory tests [38,9] while leading to an efficient computational implementation [39]. The FEM model is showcased in Fig 3.



b

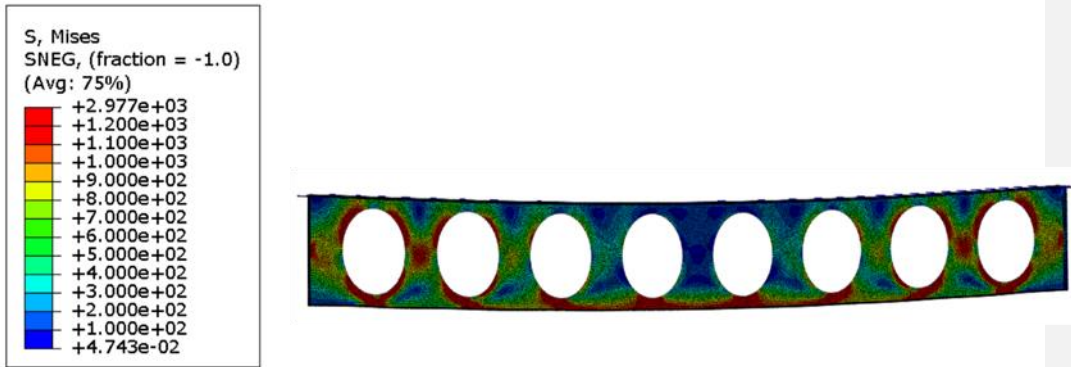


Fig 3. Overall view of the FEM model. Displacements (a) and Von Misses stresses are observed for the following test case: $L=5000\text{mm}$, $t_f=10\text{mm}$, $t_w=10\text{mm}$, $H_w=500\text{mm}$, $D_o=400\text{mm}$, $W_P=200\text{mm}$, $t_c=100\text{mm}$, $b_c=1000\text{mm}$

Gesamtansicht des FEM-Modells.

An elastic, isotropic constitutive model was employed for representing both materials, unconfined concrete, and structural steel. This is a suitable choice as deflections during operation are of interest. The following elastic parameters were considered for its definition; steel Young's modulus of 200GPa; concrete Young's modulus of 31GPa in accordance to the Eurocode 2 [40]; Poisson ratio of 0.3 for steel, and Poisson ratio of 0.2 for concrete.

Boundary conditions are presented in Fig 4. Out of plane displacements at the supports were constrained by restricting displacements at the four corners of the beam's ends, while allowing for in-plane rotations. Axial displacements were restricted on the leftmost support, while allowing them on the rightmost, representing simple and roller supports, respectively.

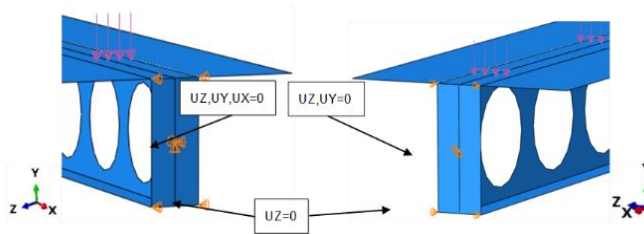


Fig. 4 Boundary conditions. Leftmost support on the left, rightmost on the right.

Randbedingungen. Ganz links Auflager, ganz rechts Auflager.

Computation of analytical deflections according to Equation (5) was done numerically considering the trapezoidal rule [41] for a given set of parameters, thus allowing for evaluation of relative errors between them and values found through FEM analyses, as shown by Equation (9)

$$E = \sum_{i=1}^N \left(1 - \frac{u_{ai}}{u_{femi}}\right)^2 \quad (9)$$

Where u_{ai} are the analytical deflections at the i -th sampling location for a given test case, while u_{femi} is the deflection according to the FEM model at the same place. The summation is done through all sampling locations of a particular test case.

It is then possible to find the set of parameters for the proposed stiffness variation, namely γ , κ , and A_e that would lead to minimum values for E in Equation (9) for each case. This is done by applying the Mathcad implementation of the KNITRO algorithm [42].

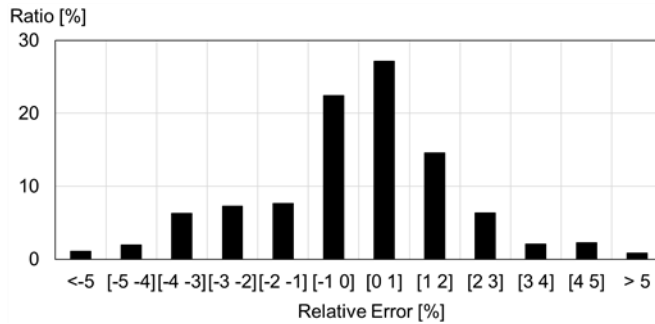


Fig. 5 Histogram of relative errors.

Histogramm der relativen Fehler.

5 Results

98% of observed errors among 1096 deflection samples range between -5% and 5%. Moreover, the 25-75% interquartile range is observed for errors ranging between -1% and 1%. Mean, median, and mode values are -0.06%, 0.06%, and 0.07% respectively, denoting how estimates are practically unbiased. Still, differences among these values show a slight skewness towards negative errors. In overall terms, results are reliable enough to assess deflections on service conditions.

The γ parameter in Equation (6) determines the oscillatory characteristics of the wavelet model [43] particularly, it takes a value of one-half of the number of openings of the cellular beams N_p setting the number of peaks of $S(\xi)$ along the beam length.

$$\gamma = \frac{N_p}{2} \quad (10)$$

Multivariate Regression Analyses allow for the definition of prediction equations for the remaining stiffness parameters, A_e , and κ in terms of geometrical characteristics of cellular beams. Specifically,

it has been observed that beam length; flange, and web thickness as well as spacing among perforations are the most relevant for defining the stiffness variation pattern. Particularly, the following expressions were found:

$$\kappa = 0.0634 - 0.0268 \frac{T_f}{T_u} - 1.1935 \frac{I_o}{bh^3} + 0.0091 \frac{L}{h} + S_{WP} \quad (11)$$

$$A_e = 0.4033 + 2.009\kappa - 0.1396 \frac{T_f}{T_u} - 1.6534 \frac{I_o}{bh^3} + 0.0566 \frac{L}{h} + S_{WP} \quad (12)$$

Where S_{WP} is a constant that takes different values depending on the narrowest thickness between perforations W_P , as shown in Fig 2. Three categories have been defined for this variable; close, for W_P values less than 35mm; average, when W_P ranges between 100 and 120mm, and; wide when W_P is larger than 200mm. The value for S_{WP} is zero for beams with average spacing, while for the other categories, it takes the quantities presented in Table 1:

Table 1 Values of S_{WP} for beams with close and large stiffener widths.

SWP-Werte für Träger mit engen und großen Rippensbreiten.

Spacing	κ	A_e
Close (< 40mm)	0.2478	0.0022
Large (>200mm)	-0.2208	0.2589

Jointly, both expressions provide a reliable way to define the stiffness variation along the length of perforated beams, as their adjusted coefficients of determination reach 0.836 for Equation (11) and 0.875 for Equation (12), making their use well-suited for design.

6 Worked Example

This example presents the design of an interior girder in the second floor of a three-level retail commercial center, which is furnished with a high-traffic, terrazzo floor. Girders are uniformly spaced 6m in both directions (NS-EW). As the girder won't be part of the lateral load support system, it will be simply supported on its framing columns. The design will be done in accordance with Eurocode 2 [7] guidelines, while loads will be prescribed by the ASCE SEI 7 [44] specifications, considering an afferent length of 6m. This leads to the design actions stated in table 2.

Table 2 Design actions considered in the example.

Berücksichtigte Bemessung Lasten des Beispiels	
Design Action	Value [kN/m]
Dead Load (W_D)	37
Live Load (W_L)	22
Ultimate Design Load ($W_u = 1.2W_D + 1.6W_L$)	80
Service Condition Load ($W_s = W_D + W_L$)	65

Loads are supported by a 500mm deep, 200mm wide 50 kSI (345 N/mm²) steel I beams that have flange and web thicknesses of 10mm; values that make the section compact for flexure [7]. It is overlaid by a $f'c = 35$ N/mm² nominal-strength 100 mm thick concrete slab furnished with shear connectors to ensure joint deformation of the slab and the beam. The required moment demand is:

$$M_u = \frac{W_u L^2}{8} = \frac{80 \times 36}{8} = 360 \text{ kNm} \quad (13)$$

The structural design will follow a simplified approach. Due to the perforations, it is assumed that only the bottom flange will contribute to the moment capacity of the cross-section. If that is the case, the maximum tensile load that can be sustained is:

$$T = A_s \cdot f_y = b \cdot t_f \cdot f_y = \frac{200 \times 10 \times 345}{1000} = 690 \text{ kN} \quad (14)$$

Where A_s is the area of the bottom flange, b is the beam width, t_f is the bottom flange thickness and f_y is the steel yield stress, 345 N/mm². Consequently, the depth of the equivalent Whitney's compressive block from the uppermost fibre of the slab is given by [45]:

$$a = \frac{T}{0.85 \cdot b_e \cdot f'c} = \frac{690000}{0.85 \times 1500 \times 28} = 16 \text{ mm} \quad (15)$$

Where b_e is the equivalent width of the concrete slab, taken as one-fourth of its length, [7]; and $f'c$ is the nominal strength of the concrete. Finally, the factored, nominal capacity of the cross-section where the perforations are the largest is at least:

$$\phi M_n = \phi \left(d - \frac{t_f}{2} + e - \frac{c}{2} \right) = 0.9 \frac{690 \times (500 - 5 + 100 - 8)}{1000} = 364 \text{ kNm} \quad (16)$$

Shear capacity of the steel beam, discarding any contribution of the slab, is:

$$\phi V_n = \phi 0.6 A_s f_y = \phi \cdot h \cdot t_w \cdot f_y = \frac{0.9 \times 0.6 \times 500 \times 10 \times 345}{1000} = 931 \text{ kN} \quad (17)$$

While, the shear demand, at the support, is:

$$V_u = \frac{w_u L}{2} = \frac{80 \times 6}{2} = 240 \text{ kN} \quad (18)$$

Thus, the shear capacity of the provided steel section is more than 3.5 times the expected demand, while it closely provides enough moment resistance, making it optimal.

The second step is the assessment of expected deflections. Firstly, the second moment of inertia of the steel beam, without perforations must be computed. For this example, it is $3.481 \times 10^8 \text{ mm}^4$. Considering the high shear over-strength available, closely spaced openings will be considered. Then, according to Equations (11,12) the κ value expected for the proposed section is:

$$\kappa = 0.0634 - 0.0268 \frac{10}{10} - 1.1935 \frac{3.481 \times 10^8}{200 \times 500^3} + 0.0091 \frac{6000}{500} + 0.2478 = 0.38 \quad (19)$$

$$A_e = 0.4033 + 2.009 \times 0.38 - 0.1396 \frac{10}{10} - 1.6534 \frac{3.481 \times 10^8}{200 \times 500^3} + 0.0566 \frac{6000}{500} + 0.0022 = 1.70 \quad (20)$$

320mm diameter of perforations are considered, the ratio H_w/D_o becomes 1.56 which is within the range specified by Equation (7). Similarly, a spacing of 300 mm between perforations leads to a ratio $S_d/D_o = 1.09$ within the boundaries stated in Equation (8). This is also within what is considered a close spacing in this study. First and last perforations will be observed at a distance of 215mm from each support, which is larger than the one-half diameter threshold that will prevent crushing due to the reaction ($D_o/2 = 160\text{mm}$), thus providing an allowance for a connection plate to the beam. In total, 16 perforations can be made through the entire length of the beam, leading to a γ value of 8. Consequently, the stiffness variation along the beam length is given by

$$S(x) = 1.70 - 0.38 \left\{ \frac{9}{16} \sin[\pi(3x - 8)] + \frac{7}{16} \sin \left[\pi \left(\frac{7}{3} x - 8 \right) \right] - \sin \left[\pi \left(\frac{8}{3} x - 8 \right) \right] \right\}^2 ;$$

$$0 \leq x \leq 6 \quad (21)$$

Where x is the beam coordinate in meters from the support. The stiffness variability obtained is depicted in figure 4. The mid deflection expected under service conditions can be obtained after evaluating the integrals in Equation (5) considering the proposed stiffness variation, and the serviceability load of 65kN/m, leading to a value of $x = 18 \text{ mm}$, which is in accord with AISC-16 [7] that set a threshold of 1/300 of the span, which for this example is 20mm.

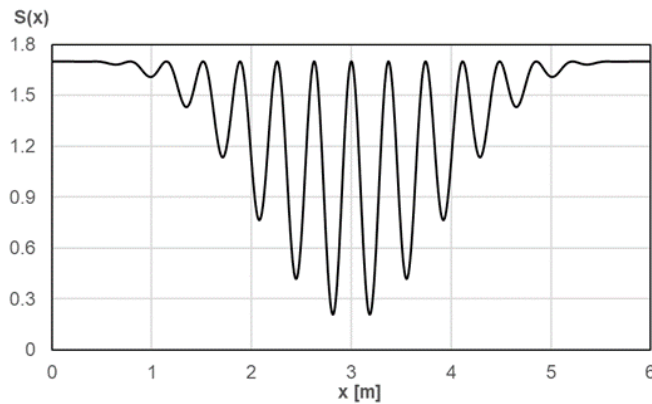


Fig. 6 Stiffness variation obtained for the example

Berechnete Steifung Variation in diesem Beispiel

7 Conclusions

This study proposes an analytical function for describing the inertia variation along the length of steel-concrete composite cellular beams. It considers a squared sum of trigonometric terms that allows for an oscillatory value of inertia that decreases when the cross-section is reduced due to the presence of openings, and then increases again when they are absent at the web-post area. The suitability of the proposed approach is verified by comparing results of deflections assessed analytically with results of more than 260 cases with varied length, spacing, web and flange thicknesses. Among more than 1000 locations where deflection was inquired, it is observed that in more than 98% of assessed locations range below 5%; while in the great majority (80%) range between -3% and +2.5%. Consequently, the proposed function is well-suited for describing the deflection of composite cellular beams when subjected to service conditions.

Furthermore, regression analyses performed on parameters that best describe this found stiffness variation pattern allow for a direct link to geometrical characteristics of steel-concrete composite perforated beams, being the most critical the number of openings, the ratio between flange and web thickness, and the inertia of the gross steel section. Obtained relationships are reliable for use by practitioners as more than 80% of variability can be explained by the proposed statistical models.

Thus, this approach provides a valuable tool for practitioners as it makes it feasible to represent the stiffness variation of steel-concrete composite perforated beams along length through a

simple mathematical expression that can be straightforwardly implemented into any structural analysis software. It is expected that this outcome will contribute to further increase the confidence in using composite and non-composite perforated beams, by easing the understanding of their deformation characteristics without requiring the use of detailed finite element models or matrix formulations. Thus, this study significantly contributes to making steel construction more sustainable by promoting a lower weight per-capita solution that makes better use of provided material.

8 Appendix

The following table shows all test cases considered in this study. For each one, all combinations of $t_f = 10, 15, \text{ and } 20$ and $t_w = 10, 15, 20$ were assessed, leading to a total of 270 models.

Table A1 Test Cases considered in this study.

In dieser Studie berücksichtigte Testfälle

Number of perforations	L [mm]	D _o [mm]
6	2960	400
	3380	
	3800	
	2466	333
	2117	286
	3392	400
7	3896	
	4400	
	2826	333
	2426	286
8	3824	400
	4412	
	5000	
	3186	333

Review

Comments

Comments

	2735	286
9	4256	400
	4928	
	5600	
	3546	330
	3044	286
10	4688	400
	5440	
	6200	
	3906	330
	286	286
11	5120	400
	5960	
	6800	
	4266	330
	3662	286

References

[1] United Nations (1987) Report of the world commission on environment and development: our shared future. Report A/42/427, General Assembly UN. New York.

[2] Boffey D. (2020). Amsterdam to embrace ‘doughnut’ model to mend post-coronavirus economy. The Guardian, 8 April 2020.

[3] Raworth K. (2017) Doughnut Economics: Seven ways to think like a 21st century economist. Chelsea Green Publishing, Chelsea VT.

[4] World Steel Association (2020) Steel’s contribution to a low carbon future and climate resilient societies. World Steel Association, Brussels, Belgium.

- [5] Oxford Economics (2017) Global Infrastructure Outlook. Global Infrastructure Hub. Sydney, Australia.
- [6] Benitez MA, Darwin D and Donahey RC (1998). Deflections of composite beams with web openings, *Journal of Structural Engineering*, 124(10), 1139-1147.
- [7] American Institute of Steel Construction, AISC. (2016) Specifications for structural steel buildings. AISC 360, Chicago, ill.
- [8] Chung K.F., Liu T.C.H. and Ko A.C.H. (2000) "Investigation on Vierendeel mechanism in steel beams with circular web openings." *Journal of Constructional Steel Research*, 57, pp. 467-490
- [9] Tsavdaridis, K.; D'Mello, C. (2009) Web buckling study of the behaviour and strength of perforated steel beams with different novel web opening shapes. *J. Constr. Steel Res.*, 67, 1605–1620
- [10] Erdal F., Saka M. (2013) Ultimate load carrying capacity of optimally design steel cellular beams. *Journal of Constructional Steel Research*, 80, 355-368
- [11] Wang P., Kangrui G., Zhang L. (2016) Shear buckling of web-post in a castellated steel beam with hexagonal we openings. . *J. Constr. Steel Res*, 121, 173-184
- [12] Tsavdaridis K., D'Melo, C. (2012) Optimization of novel-elliptically-based eb openings shapes of perforated steel beams. .*J. Constr. Steel Res*, 76 , 39-53
- [13] Tsavdaridis K., Kingman J., Toropov V. (2015) Application of structural topology optimisation to perforated steel beams. *Computers and structures*, 158, 108-123
- [14] Feng R., Zhan H., Meng S., Zhi J. (2018) Experiments on H-shaped strength steel beams with perforated web. *Engineering structures*, 177, 374-394.
- [15] Tsavdaridis K., Galiatsatos G. (2015) Assessments of cellular beams with transverse stiffeners an closely spaced web openings. *Thin-walled structures*, 94, 636-650.
- [16] Tsavdaridis K., D'Mello C., Huo, B. (2013). Experimental and computational study of the vertical shear behaviour of partially encased perforated steel beams. *Engineering structures*, 56, 805-822.
- [17] Ahmed I. and Tsavdaridis K. (2018) Life cycle assessment (LCA) and cost (LCC) studies of lightweight composite flooring systems. *Journal of building engineering*, 20,.624-633.

- [18] Maraveas C. (2017) Fire resistance of DELTABEAM® composite beams: a numerical investigation. *Journal of Structural Fire Engineering*, 8 (4), 338-353.
- [19] Akrami V., and Erfani S. (2016) Review and assessment of design methodologies for perforated steel beams. *Journal of Structural Engineering*, 142 (2), 1-14.
- [20] Sonck D, Kinget L and Belis J (2015). Deflections of cellular and castellated beams. *International Association for Shell and Spatial Structures (Symposium 2015)*. 17-20 August 2015, Amsterdam, Netherlands.
- [21] Lawson RM, Hicks SJ (2011). Design of composite beams with large openings SCI P355, Steel Construction Institute, Berkshire, UK.
- [22] Charleson A (2007) Architectural design for earthquake, a guide to the design of non-structural elements. New Zealand society for earthquake engineering, Wellington.
- [23] Magenes G, Modena C, Da Porto F, Morandi P (2009) Behavior and design of new masonry buildings: recent developments and consequent effects of design codes. In: Eurocode 8 perspectives from the Italian perspective workshop. Doppiavoce, Napoli, pp 199–212.
- [24] Dougherty BK (1980). Elastic deformation of beams with web opening, *Journal of the Structural Division*, ASCE 106(1), 301-312.
- [25] Donahey RC and Darwin D (1986). Performance and design of composite beams with web openings AISC Research project 21.82, American Institute of Steel Construction.
- [26] Darwin D (1990). Steel and composite beams with web openings (AISC Design Guides), American Institute of Steel Construction.
- [27] Ward JK (1990). Design of composite and non-composite cellular beams SCI P100, Steel Construction Institute, Berkshire UK.
- [28] Muller C, Hechler O, Bureau A, Bitar D, Joyeux D, Cajot LG, Demarco T, Lawson RM, Hicks S, Devine P, Lagerqvist O, Hedmann-Petursson E, Unosson E, Feldmann M (2006). Large web openings for service integration in composite floors, European Communities, Luxembourg.
- [29] Zhou D, Li L, Schnell J, Kurz W and Wang P (2012). Elastic deflections of simply supported steel I-beams with a web opening, *Procedia Engineering*, 31(2012), 315-323.

- [30] Panedpojaman P and Thepchatri T (2013). Finite element investigation on deflection of cellular beams with various configurations, *International Journal of Steel Structures*, 13(3), 487-494.
- [31] Daubechies I. (1992) Ten lectures on wavelets. SIAM: Society for Industrial and Applied Mathematics. Philadelphia, PA.
- [32] Goodman R. (2006) Discrete Fourier and wavelet transforms: an introduction through linear algebra with applications to signal processing. WSPC World Scientific. Singapore.
- [33] Makris N., Vassiliou M. (2011) Estimating time scales and length scales in pulselike earthquake acceleration records with wavelet analysis. *Bulletin of the Seismological Society of America*. 101 (2) : 596-618.
- [34] Hibbeler R. (2016) Mechanics of materials. 10th Edition. Pearson. London, UK.
- [35] Alonso-Rodriguez, Miranda E. (2015) Assessment of building behavior under near-fault pulse-like ground motions through simplified models. *Soil Dynamics and Earthquake Engineering*, 79 : 47-58.
- [36] Smith M. (2009) Abaqus/standard user's manual. Edition 6.9. Dassault Systèmes Simulia Corp, Providence, RI.
- [37] El-Sawhy, K.L.; Sweedan, A.M.I.; Martini, M.I. Moment gradient factor of cellular steel beams under inelastic flexure. *J. Constr. Steel Res.* 2014, 98, 20–34.
- [38] Surtees, J.O.; Lui, Z. (1995) Report of Loading Tests on Cellform Beams; University of Leeds: Leeds, UK.
- [39] Abambres, M., Rajana, K., Tsavdaridis, K. and Ribeiro, T., 2018. Neural Network-Based Formula for the Buckling Load Prediction of I-Section Cellular Steel Beams. *Computers*, 8(1), p.2.
- [40] European Committee for Standardization CEN (2002) Eurocode 2: design of concrete structures – part 1-1: general rules and rules for buildings. Brussels, Belgium.
- [41] Kreyszig E. (2017) Advanced engineering mathematics, 10th edition. Wiley, Hoboken NJ, USA.
- [42] Byrd R., Nocedal J., Waltz, R. (2006) Knitro: an integrated package for non-linear optimization; in Large scale non-linear optimization: 35-59. Springer; Berlin Germany.

- [43] Mavroeidis G and Papageorgiou AS (2003). A mathematical representation of near-fault ground motions, *Bulletin of the Seismological Society of America*, 93(3), 1099-1131.
- [44] American Society of Civil Engineers (2016) Minimum design loads for buildings and other structures. ASCE, 3rd Ed. Reston VA.
- [45] Darwin D., Dolan C., Nilson A. (2015) Design of concrete structures. Mc-Graw Hill education, 15th Ed. New York, NY.

Authors

Komal Rajana

City University of London

School of Mathematics, Computer Science and Engineering

Northampton Square

London, UK EC1V 0HB

komal_rajana@hotmail.com

Corresponding Author:

Dr. Andrés Alonso-Rodríguez

Assistant Professor

University of Nottingham at Ningbo

Faculty of Science and Engineering

199 Taikang East Road

Ningbo, China; 315100

andalon@gmail.com

Review

Comments

Comments

Dr. Konstantinos Daniel Tsavdaridis

Associate Professor

University of Leeds

School of Civil Engineering

Faculty of Engineering and Physical Sciences

Woodhouse Lane, West Yorkshire

Leeds, UK. LS2 9DY

K.Tsavdaridis@leeds.ac.uk

Review

Comments

Comments